# Solid-solid phase transitions and phonon softening in an embedded-atom method model for iron

Luis Sandoval,[1] Herbert M. Urbassek,[1,*] and Peter Entel[2]
[1]*Fachbereich Physik und Forschungszentrum OPTIMAS, Universität Kaiserslautern, Erwin-Schrödinger-Straße, D-67663 Kaiserslautern, Germany*
[2]*Fachbereich Physik und CeNIDE, Universität Duisburg-Essen, Lotharstraße 1, D-47048 Duisburg, Germany*
(Received 17 July 2009; published 10 December 2009)

We show theoretical results concerning solid-solid phase transitions in Fe induced by pressure at 0 K and by temperature at 0 GPa. One intermediate case for 300 K at 9.8 GPa is also considered. The interatomic potential employed has been shown to be capable of describing the martensite-austenite phase transition in iron. We study the phonon dispersion curves at 0 K, and their variation by pressure. After identifying a soft phonon mode, we determine the transition pressure using several techniques. From molecular-dynamics simulations we obtain the phonon dispersion curves for 0 and 9.8 GPa at 300 K. We also study the phonon softening by temperature. We find the vibrational Gibbs free energy and compare the transition temperature with the value found by using thermodynamic integration. A calculation of the vibrational entropy demonstrates that the inclusion of anharmonicities beyond the quasiharmonic approximation has only a minor effect (10%).

DOI: 10.1103/PhysRevB.80.214108 PACS number(s): 65.40.gd, 61.50.Ks, 63.20.−e, 64.70.kd

## I. INTRODUCTION

There are, at least, four known allotropes, or more precisely, three enantiotropic modifications of iron.[1,2] Ferromagnetic $\alpha$-Fe (ferrite) with a bcc crystal structure is stable at room temperature and ambient pressure. When the temperature is increased, it transforms to an fcc structure at 1184 K, called $\gamma$-Fe or austenite. By keeping the pressure at 0 GPa, the crystal structure changes again to a bcc structure, also called $\delta$-Fe, at 1665 K, before melting at 1811 K. Increase in pressure induces another solid-solid phase transition; at room temperature, the bcc phase transforms at $\sim$13 GPa to an hcp phase, which is called $\epsilon$-Fe. There is no $\beta$-Fe because of a mistake: previously it was thought that the phase between the Curie point, 1043 K, and the $\alpha$-$\gamma$ transition point, 1184 K, where paramagnetic bcc Fe is stable, was a different allotrope (and the name $\beta$-Fe was assigned to that phase). The complexity of Fe regarding structural transformation even increases when considering various steels since alloying Fe with other transition and tracer elements makes the interplay of magnetism and structure very subtle as, for instance, in the case of Fe-Mn steels where antiferromagnetism competes with ferromagnetic order.[3]

It is not easy to capture such an allotropy with the help of *empirical interatomic potentials* in a reliable model to use in molecular-dynamics simulations. Usually the models, mainly in the embedded-atom method (EAM) approach, are fitted to low-temperature properties at ambient pressure, and hence to the bcc phase. Examples are: crack propagation in $\alpha$-Fe,[4] solid-liquid interfaces,[5] magnetism in $\alpha$-Fe,[6] Fe-Ni alloys,[7–9] self-diffusion of adatoms on the bcc-Fe(100) surface,[10] threshold displacement energies,[11] interface dynamics,[12] shock waves,[13] and carbon diffusion in $\alpha$-Fe.[14] Only a few potentials have shown the capability to reproduce a solid-solid phase transition in Fe, such as the Meyer-Entel potential[7] or the Müller *et al.*[15] potential, which is of the bond-order type. Given the importance, theoretical and practical, of these phase transitions, it is desirable to test the transferability of these potentials to new physical situations.

Multimillion atom simulations of dynamic processes require reliable empirical many-body potentials. For the simulation of solid-state phase transitions, these potentials need to implement the small energetic differences of the various relevant lattice structures. In addition, the temperature (and pressure) dependence of the vibronic properties of the lattices including their entropy contributions are important as they ultimately determine the phase-transition point. For a material such as Fe, where magnetism gives an important—if not the decisive—contribution to the interatomic forces, the generation of an effective classical interatomic potential is particularly challenging.

In this contribution we want to explore the capability of an EAM potential to describe the physics of solid-solid phase transitions in a realistic way. To this end, we explore the properties of bcc iron both with respect to temperature and pressure increase; we show results for the pressure-induced transition at 0 K and for the temperature-induced transition at 0 GPa. A temperature of 300 K at 9.8 GPa was also considered due to the availability of experimental data. We have used the Meyer-Entel potential[7] due to its computational convenience; it is fast enough to allow simulations of systems with millions of atoms for long-time intervals on the order of nanoseconds using modest computational resources, and it has already produced good results for pure iron and nickel ferrous alloys.[7,13,16–18] First of all we study the phonon dispersion curves at 0 K, and their variation by pressure. After identifying a soft phonon mode, we find the transition pressure using various techniques. From molecular-dynamics simulations we obtain the phonon-dispersion curves for 0 and 9.8 GPa at 300 K. We also study the phonon softening induced by temperature. We evaluate the vibrational Gibbs free energy and compare the transition temperature with the value found by using the *metric-scaling* technique[19] applied to a particular transformation path.

## II. PRESSURE DEPENDENCE OF STRUCTURAL TRANSFORMATION IN IRON

In Fig. 1 we show the phonon-dispersion curves for 0 and 9.8 GPa at 0 K, which were calculated by solving the dy-

 

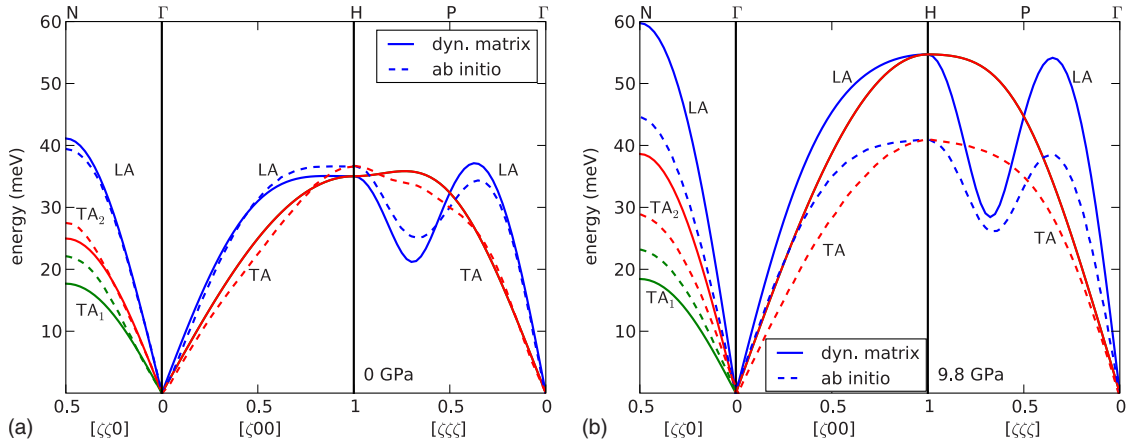


FIG. 1. (Color online) Phonon-dispersion curves of bcc iron for (a) 0 and (b) 9.8 GPa at 0 K calculated from the dynamical matrix using the EAM potential. We include *ab initio* data from Refs. 20 and 21 for 0 and 9.8 GPa, respectively.

namical matrix[22] along three high symmetry directions in the Brillouin zone. A comparison of the zero-pressure phonon dispersions obtained from the EAM model with up to date first-principles calculations[20,23] and inelastic neutron-scattering data at room temperature[24–26] shows very good agreement. (An estimate of zero-point motion and thermal effects on the calculated generalized gradient approximation (GGA) phonon dispersions can be found in Ref. 23. The conclusion is that GGA tends to slightly underestimate the phonon frequencies if thermal effects are taken into account.) It is obvious from the experimental, *ab initio* as well as EAM results that the zero-temperature or room-temperature phonon dispersions in the bcc structure do not show a trace of phonon softening. This has been attributed to the influence of magnetism in stabilizing the more open bcc (compared to fcc) crystal lattice structure. Even above the Curie temperature, we still find persisting local magnetic moments in the paramagnetic phase which may help to stabilize the bcc structure until finally entropic contributions favor the fcc lattice above 1184 K. Since the EAM potentials are fitted to the elastic properties of the low-temperature magnetic state of iron, they are able to mimic to some degree the influence of magnetism on stabilizing the bcc structure. The subtle interplay of vibronic, electronic, and magnetic contributions to the *ab initio* free energy of iron at finite temperatures and zero pressure has recently been discussed in Ref. 20. Analogous calculations for still higher temperatures are necessary in order to finally settle the question why the vibrational entropic contributions change iron back to the bcc structure ($\delta$ phase) just before melting. In the absence of external pressure, any softening of the vibrational spectrum of iron, if at all visible in the phonon dispersions, will be restricted to the intermediate neighborhood of the structural transitions itself. This observation does not contradict the finding that the shear $TA_1$ mode has rather low frequency and under pressure or alloying may initiate the so-called martensitic transformation as in the binary Fe-Ni, Fe-Pt, and Fe-Pd systems.

The increase in pressure produces a broadening in the energy range, which is clearer seen in the density of states plotted in Fig. 2. Such an enhancement has also been observed in experiments,[26] but the results from the EAM potential show an excessive effect (about 50%), which can be explained by the high anharmonicity that this potential exhibits.[19] Nevertheless, it is interesting to note the behavior of the $TA_1$ branch, whose role as transformation precursor in martensitic transformation has been highlighted, with some caution, previously.[26–29] In Fig. 3 we show the $\frac{1}{2}TA_1[110]$ phonon mode as a function of the pressure at 0 K. Although the restoring force associated to this mode vanishes at 132 GPa, the transition may take place at a lower pressure,[30] since the lattice may become thermodynamically unstable before the onset of mechanical instability. In order to find the true transition pressure for the Meyer-Entel potential we use the enthalpy $h$ (per atom) given by

$$h = e + Pv_{\mathrm{at}}, \tag{1}$$

which may be calculated analytically. Here $e$ is the internal energy per atom and $v_{\mathrm{at}}$ is the atomic volume. The corresponding data are shown in Fig. 4 in the form of the enthalpy differences of the fcc and hcp phases with respect to the bcc phase. The bcc phase is stable at low pressures up to 53 GPa. For larger pressures, the fcc phase starts to show the lowest enthalpy. The hcp phase is nowhere stabilized. In ex-

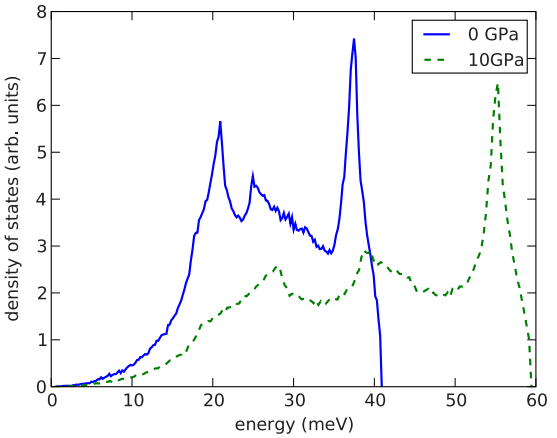


FIG. 2. (Color online) Phonon density of states for bcc iron for 0 and 9.8 GPa at 0 K.

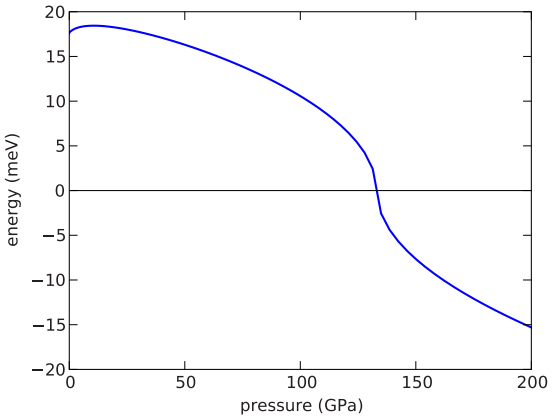


FIG. 3. (Color online) $\frac{1}{2}$TA$_1$[110] phonon mode as a function of pressure at 0 K. Negative values of the energy indicate imaginary eigenvalues of the dynamical matrix.

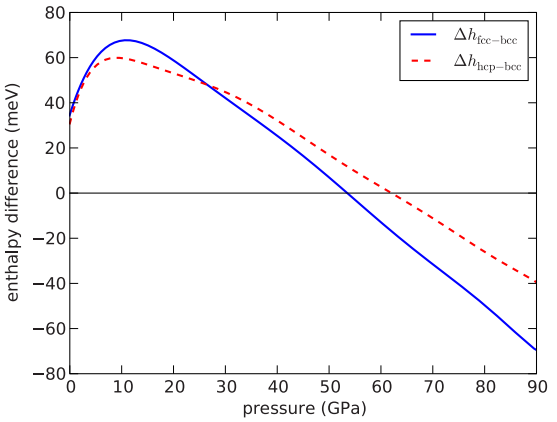


FIG. 4. (Color online) Enthalpy differences per atom of the fcc and hcp phases with respect to the bcc phase of Fe at 0 K.

periment, however, Fe transforms from the low-pressure bcc phase to hcp rather than to fcc; furthermore the experimental transition pressure is ~13 GPa (Ref. 31) and thus considerably lower than the transition pressure predicted by the EAM potential. This shows that the EAM potential studied here is not completely transferable to high values of pressure. Note that in the fitting procedure of the EAM potentials, the bcc lattice and its bcc typical arrangement of nearest and second nearest neighbors was used, which means that the EAM potential will not accurately take care of the distribution of the valence-electron charge in a typical fcc environment.[7] In any case, a qualitative comparison would be useful to gain insight in the transformation process.

We note that this transition point can also be calculated using the common-tangent technique.[32] If we plot the $e(v_{\mathrm{at}})$ curves for two phases, the negative of the slope of the common tangent line may be taken as the transition pressure. The results agree with those reported above.

## III. TEMPERATURE DEPENDENCE OF STRUCTURAL TRANSFORMATION IN IRON

We have also made a similar study for the phase transition induced by temperature. We start by calculating the phonon-dispersion curves via a molecular-dynamics approach. Our cubic simulation box consists of 12 and 10 unit cells per cube side for the bcc and fcc crystal structures, respectively, with periodic boundary conditions. After 50 ps of equilibration by means of a Nosé-Hoover thermostat, the system is left free to evolve in the microcanonical ensemble for another 50 ps. We monitor the atom velocities with a sampling rate of 100 THz for time intervals of 20.48 ps, thus generating 2048 values. The statistical average is made by shifting the initial point of this interval 2000 times.

In Fig. 5, we show the phonon dispersion curves at 300 K for 0 and 9.8 GPa, which were obtained from the velocity autocorrelation function (VACF) in the reciprocal space.[33,34] Specifically, for a given polarization $p$, the autocorrelation function is defined as

$$A^p(\mathbf{k},t) = \frac{\langle v^p_{\mathbf{k}}(t) v^p_{\mathbf{k}}(0)\rangle}{\sum_p \langle v^p_{\mathbf{k}}(0) v^p_{\mathbf{k}}(0)\rangle}, \tag{2}$$

where $v^p_{\mathbf{k}}(t) = \Sigma_j v^p_j(t) e^{-i\mathbf{k}\cdot\mathbf{r}_j(t)}$, $\mathbf{k}$ is the corresponding wave vector, $v^p_j$ is the projection of the velocity of atom $j$ on the

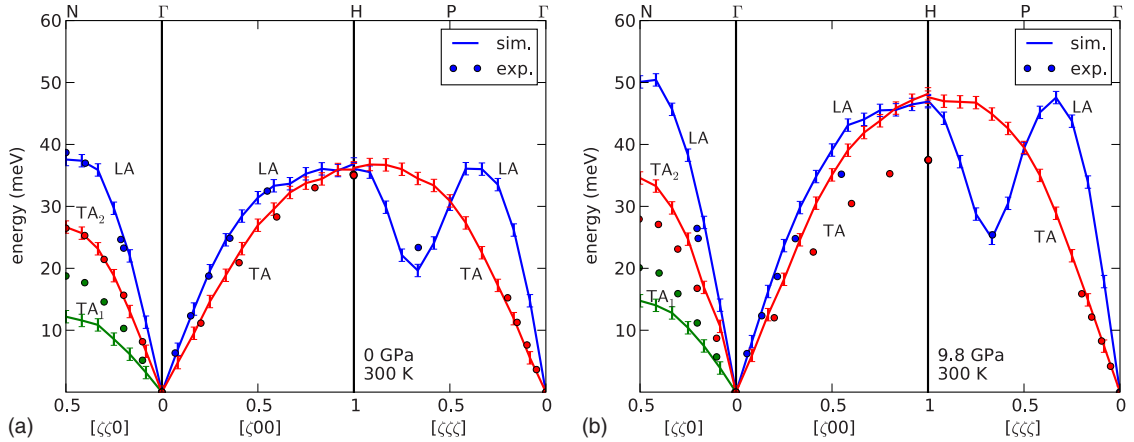


FIG. 5. (Color online) Phonon-dispersion curves of bcc iron at 300 K for (a) 0 and (b) 9.8 GPa. Experimental data taken from Ref. 26.

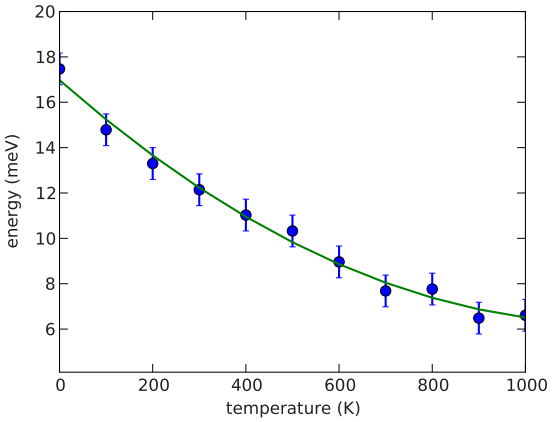


FIG. 6. (Color online) $\frac{1}{2}$TA$_1$[110] phonon mode in bcc Fe as a function of temperature at 0 GPa.

corresponding polarization vector, and $\mathbf{r}_j$ its position. By means of the Fourier transform of $A^p(\mathbf{k},t)$ we can find the corresponding eigenfrequencies from the locations of the peaks. Since the EAM potential was fitted to some selected phonon modes,[7] the agreement with the experimental values is good for 0 GPa,[25,26] with the exception of the TA$_1$[110] branch. However, we observe in Fig. 5 that for the higher pressure, 9.8 GPa, the calculated phonon-dispersion curves show an excessive enhancement in their frequency range; this behavior is analogous to the 0 K case when applying pressure, cf. Figs. 1 and 2. One reason for this unphysical enhancement of modes in iron under pressure is connected with the fact that the elastic behavior of the material under pressure is not considered when fitting the EAM potential, i.e., the total EAM energy as a function of the volume/atom does, for volumes smaller than the equilibrium volume, not agree with the volume variation in *ab initio* total-energy curves. We have found that it seems to be extremely difficult to get rid of this artifact of the EAM potentials for Fe; possibly, one would get a better EAM potential in presence of pressure if an explicit magnetic term would be available for the fitting.

In Fig. 6 we show the $\frac{1}{2}$TA$_1$[110] phonon mode as a function of temperature, where we can observe a progressive softening, but without vanishing. This result is similar to our previous observations in the pressure-induced phase transition, where we saw a progressive softening below the transition pressure, cf. Figs. 3 and 4. This behavior is in agreement with *ab initio*[30] and experimental[28] results, which also shows that the $\frac{1}{2}$TA$_1$[110] phonon mode does not vanish at the transition point.

In Fig. 7, we show a contour plot of the phonon density of states (DOS) as a function of temperature for the bcc and fcc phases at 0 and 9.8 GPa. We obtained these data by calculating the VACF in real space defined as

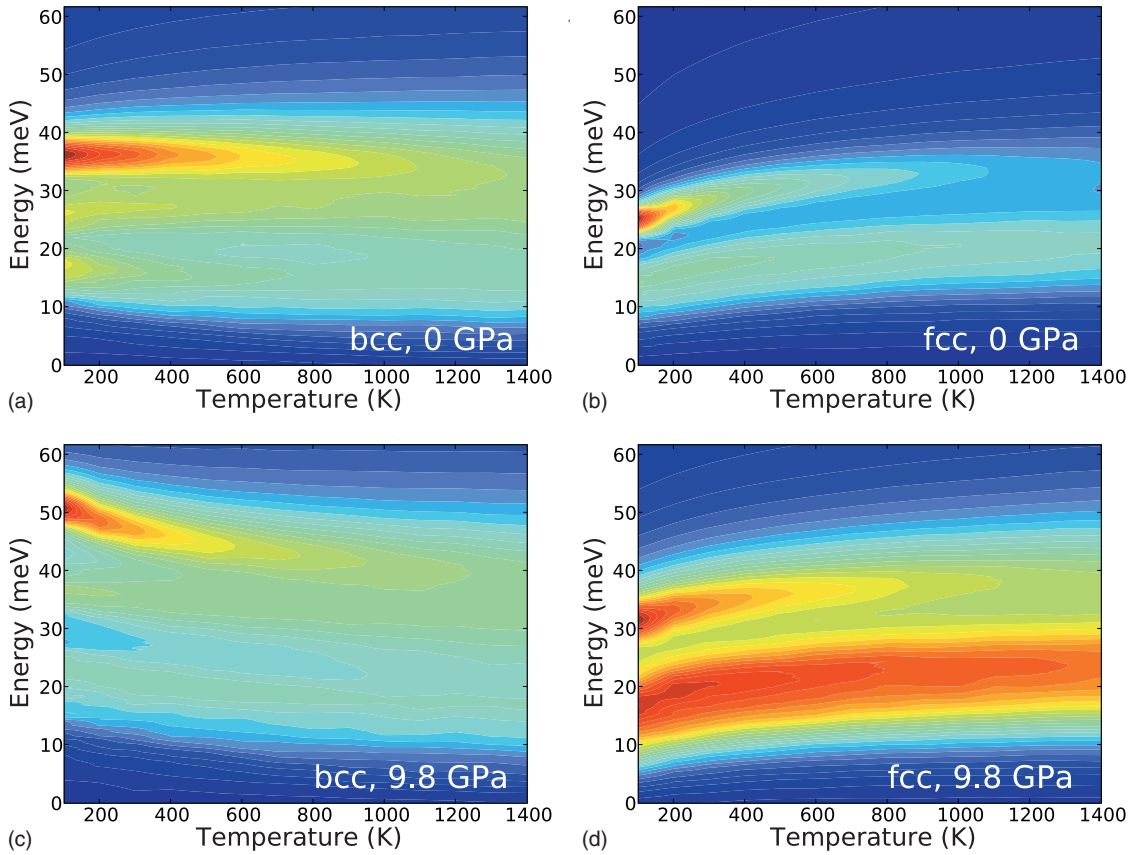


FIG. 7. (Color) Phonon density of states of Fe as a function of temperature. The Fe phase and the pressure are indicated in the figures. The colors, from blue to red, denote the height of the DOS in arbitrary units.

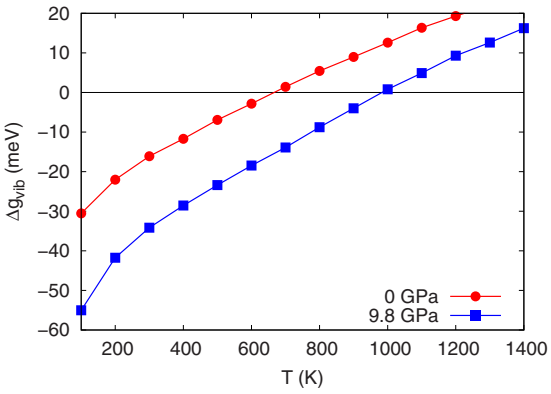


FIG. 8. (Color online) Vibrational free-energy difference for iron at 0 and 9.8 GPa.

$$\gamma(t) = \frac{\left\langle \sum_j \mathbf{v}_j(t) \cdot \mathbf{v}_j(0) \right\rangle}{\left\langle \sum_j \mathbf{v}_j(0) \cdot \mathbf{v}_j(0) \right\rangle}. \tag{3}$$

By using the Fourier transform of the VACF, we obtain the phonon density of states $D(\omega)$ with an (angular-frequency) resolution of 0.31 THz and a cut-off angular frequency $\omega_c$ of 314 THz. We normalize the phonon density of states $D(\omega)$ as follows:

$$\int_0^{\omega_c} D(\omega) d\omega = 1. \tag{4}$$

In Fig. 7, we notice an obvious suppression of sharp peaks and an enhancement in the frequency range with temperature in all cases. The bcc phase is shifted to higher frequencies under pressure, which is more notable at lower temperatures, while the fcc phase shows an increasing contribution in the lower frequency range with pressure.

## IV. ENTROPIC CONSIDERATIONS

In this section, we proceed in another way in order to identify the stability of the lattice structures and the transition temperatures. For this purpose, we use the quasiharmonic approach and calculate the vibrational Gibbs free-energy difference per atom between the bcc and the fcc phases given by

$$\Delta g_{\mathrm{vib}} = g_{\mathrm{vib}}^{\mathrm{bcc}} - g_{\mathrm{vib}}^{\mathrm{fcc}} = \Delta e - T\Delta s_{\mathrm{vib}} + P\Delta v_{\mathrm{at}}. \tag{5}$$

Here, $\Delta e$ is the internal-energy difference between the bcc and the fcc phases, $\Delta s_{\mathrm{vib}}$ is the vibrational entropy difference per atom, and $\Delta v_{\mathrm{at}}$ is the difference in atomic volumes for bcc and fcc at pressure $P$. The quasiharmonic expression for the vibrational entropy is given by an integral over the density of states $D(\omega)$

$$\frac{s_{\mathrm{vib}}}{k_B} = -3 \int d\omega D(\omega) \{ n(\omega) \ln n(\omega) - [n(\omega)+1] \ln[n(\omega)+1] \}, \tag{6}$$

where the number of phonons is determined by $n(\omega) = (e^{\hbar\omega/k_B T} - 1)^{-1}$.[35]

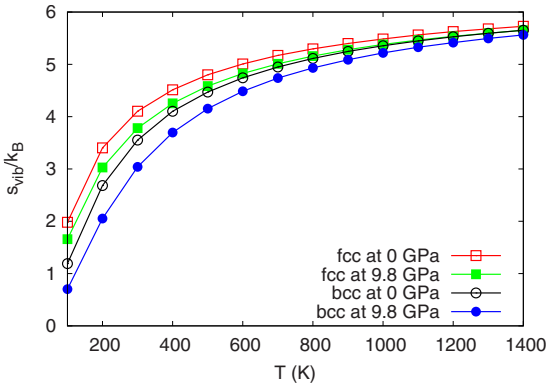


FIG. 9. (Color online) Vibrational entropy $s$ for bcc and fcc iron at 0 and 9.8 GPa as a function of temperature, calculated in the quasiharmonic approximation, Eq. (6).

In Fig. 8, the Gibbs free-energy difference is shown, which was calculated using Eq. (5). We obtain transition temperatures of 670 and 990 K for 0 and 9.8 GPa, respectively. In our previous work,[19] we have calculated the transition temperature at 0 GPa via thermodynamic integration and obtained a value of $550 \pm 50$ K, which is in acceptable agreement with the value found here. The relative deviations to the experimental results are 43% for 0 GPa [exp. 1184 K (Ref. 31)] and 27% [exp. 780 K (Ref. 31)] for 9.8 GPa. Note, however, that in our potential pressure increase stabilizes the bcc phase and increases the $\alpha/\gamma$ transition pressure, while the reverse is true in experiment.[1]

Figure 9 shows the vibrational entropy for iron in the bcc and fcc phases at 0 and 9.8 GPa as a function of temperature, as calculated by Eq. (6), while Fig. 10 shows the vibrational entropy differences between the fcc and the bcc phases. At the temperatures, where the transition from bcc to fcc occurs, we obtain entropy differences of 0.23 and $0.16 k_B$/atom, for 0 and 9.8 GPa, respectively. At the transition point, the vibrational entropy difference has been determined experimentally at 0 GPa as $0.14 k_B$/atom (Ref. 28); this value is in reasonable agreement with our result. Note that the experimental

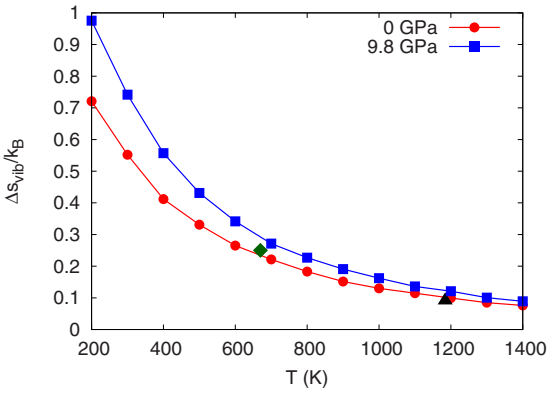


FIG. 10. (Color online) Vibrational entropy difference between the fcc and bcc phases at 0 and 9.8 GPa, calculated in the quasiharmonic approximation, Eq. (6). Green rhombus: total vibrational entropy difference, including anharmonicity, Eq. (5), at the theoretical phase-transition temperature. Black triangle: experimental value at the phase-transition temperature (Ref. 36).

result led to the conclusion that the vibrational contribution is larger than the electronic contribution to entropy, and that it is therefore the excess of vibrational entropy which stabilizes the high-temperature phase.[28]

Immediately at the transition point, Eq. (5) allows to determine the entropy difference accurately from a measurement of the internal energies (or enthalpies). For the EAM potential this gives a value at 0 GPa of $0.25k_B$/atom, in contrast to the quasiharmonic result of $0.23k_B$/atom noted above. This comparison immediately demonstrates that the inclusion of anharmonicities beyond the quasiharmonic level has only a minor effect for the accurate evaluation of the entropy.

## V. CONCLUSIONS

In this work, we have tested the transferability of an EAM potential, which is capable of describing—at least semiquantitatively—the martensite-austenite phase transition in iron. An increase in pressure produces a broadening in the energy range shown in the phonon-dispersion curves. Although such an enhancement is seen in experiments,[26] the results obtained from the EAM potential show an excessive effect (about 50%); we explain this feature by the elastically too hard behavior of the EAM potential at volumes smaller than the equilibrium volume of iron.[19] We have observed a progressive phonon softening, but without complete vanishing, in both the pressure-induced and the temperature-induced phase transitions. This behavior is in agreement with *ab initio*[30] and experimental results of phonon measurements at elevated temperatures[28] showing that the $\frac{1}{2}\mathrm{TA}_1[110]$ phonon mode does not vanish at the transition point. Finally, we demonstrate that the inclusion of anharmonicities beyond the quasiharmonic approximation has only a minor effect (10%) in the calculation of the vibrational entropy. In summary, we have demonstrated that the EAM potential considered is within the limits indicated in this study well capable to be used in qualitative studies of the solid-solid phase transitions of Fe.

## ACKNOWLEDGMENT

The authors acknowledge support by the Deutsche Forschungsgemeinschaft via the Graduiertenkolleg 814.

*urbassek@rhrk.uni-kl.de; http://www.physik.uni-kl.de/urbassek/

[1] H. Hasegawa and D. G. Pettifor, Phys. Rev. Lett. **50**, 130 (1983).
[2] G. Chen and T. J. Ahrens, Geophys. Res. Lett. **22**, 21 (1995).
[3] W. Pepperhoff and M. Acet, *Constitution and Magnetism of Iron and Its Alloys* (Springer, Berlin, 2001).
[4] A. Latapie and D. Farkas, Phys. Rev. B **69**, 134110 (2004).
[5] D. Y. Sun, M. Asta, J. J. Hoyt, M. I. Mendelev, and D. J. Srolovitz, Phys. Rev. B **69**, 020102(R) (2004).
[6] S. L. Dudarev and P. M. Derlet, J. Phys.: Condens. Matter **17**, 7097 (2005).
[7] R. Meyer and P. Entel, Phys. Rev. B **57**, 5140 (1998).
[8] Y. Mishin, M. J. Mehl, and D. A. Papaconstantopoulos, Acta Mater. **53**, 4029 (2005).
[9] G. Bonny, R. C. Pasianot, and L. Malerba, Modell. Simul. Mater. Sci. Eng. **17**, 025010 (2009).
[10] H. Chamati, N. I. Papanicolaou, Y. Mishin, and D. A. Papaconstantopoulos, Surf. Sci. **600**, 1793 (2006).
[11] K. Nordlund, J. Wallenius, and L. Malerba, Nucl. Instrum. Methods Phys. Res. B **246**, 322 (2006).
[12] C. Bos, J. Sietsma, and B. J. Thijsse, Phys. Rev. B **73**, 104117 (2006).
[13] K. Kadau, T. C. Germann, P. S. Lomdahl, R. C. Albers, J. S. Wark, A. Higginbotham, and B. L. Holian, Phys. Rev. Lett. **98**, 135701 (2007).
[14] K. Tapasa, Y. Osetsky, and D. Bacon, Acta Mater. **55**, 93 (2007).
[15] M. Müller, P. Erhart, and K. Albe, J. Phys.: Condens. Matter **19**, 326220 (2007).
[16] P. Entel, K. Kadau, R. Meyer, H. C. Herper, M. Acet, and E. F. Wassermann, J. Magn. Magn. Mater. **177-181**, 1409 (1998).
[17] P. Entel, R. Meyer, and K. Kadau, Philos. Mag. B **80**, 183 (2000).
[18] C. Engin and H. M. Urbassek, Comput. Mater. Sci. **41**, 297 (2008).
[19] C. Engin, L. Sandoval, and H. M. Urbassek, Modell. Simul. Mater. Sci. Eng. **16**, 035005 (2008).
[20] F. Körmann, A. Dick, B. Grabowski, B. Hallstedt, T. Hickel, and J. Neugebauer, Phys. Rev. B **78**, 033102 (2008).
[21] H. C. Hsueh, J. Crain, G. Y. Guo, H. Y. Chen, C. C. Lee, K. P. Chang, and H. L. Shih, Phys. Rev. B **66**, 052420 (2002).
[22] M. S. Daw and R. D. Hatcher, Solid State Commun. **56**, 697 (1985).
[23] A. Dal Corso and S. de Gironcoli, Phys. Rev. B **62**, 273 (2000).
[24] B. N. Brockhouse, H. E. Abou-Helal, and E. D. Hallman, Solid State Commun. **5**, 211 (1967).
[25] V. J. Minkiewicz, G. Shirane, and R. Nathans, Phys. Rev. **162**, 528 (1967).
[26] S. Klotz and M. Braden, Phys. Rev. Lett. **85**, 3209 (2000).
[27] R. A. Cowley, Phys. Rev. B **13**, 4877 (1976).
[28] J. Neuhaus, W. Petry, and A. Krimmel, Physica B (Amsterdam) **234-236**, 897 (1997).
[29] P. Entel, K. Kadau, R. Meyer, V. Crisan, H. Ebert, T. C. Germann, P. S. Lomdahl, and B. L. Holian, Adv. Solid State Phys. **40**, 345 (2000).
[30] M. Ekman, B. Sadigh, K. Einarsdotter, and P. Blaha, Phys. Rev. B **58**, 5296 (1998).
[31] F. P. Bundy, J. Appl. Phys. **36**, 616 (1965).
[32] M. T. Yin and M. L. Cohen, Phys. Rev. B **26**, 5668 (1982).
[33] P. Heino, Eur. Phys. J. B **60**, 171 (2007).
[34] N. I. Papanicolaou, I. E. Lagaris, and G. A. Evangelakis, Surf. Sci. **337**, L819 (1995).
[35] U. Pinsook, Phys. Rev. B **66**, 024109 (2002).
[36] Q. Chen and B. Sundman, J. Phase Equilib. **22**, 631 (2001).